Advancing Neutron Detection: Fabrication, Characterization, and Performance Evaluation of Self-Powered PIN BGaN/GaN Superlattice-Based Neutron Detectors

Ashutosh Srivastava, Adama Mballo, Suresh Sundaram, Vishnu Ottapilakkal, Phuong Vuong, Soufiane Karrakchou, Mritunjay Kumar, Xiaohang Li, Yacine Halfaya, Simon Gautier, et al.

Advancing Neutron Detection: Fabrication, Characterization and Performance Evaluation of Self-Powered PIN BGaN/GaN Superlattice Based Neutron Detectors

Ashutosh Srivastava[1,3], Adama Mballo[1], Suresh Sundaram[1,2,3], Vishnu Ottapilakkal[1], Phuong Vuong[1,3], Soufiane Karrakchou[1], Mritunjay Kumar[4], Xiaohang Li[4], Yacine Halfaya[5], Simon Gautier[5], Paul L. Voss [1,2], Jean Paul Salvestrini[1,2,3] and Abdallah Ougazzaden[1,2]

[1] CNRS, IRL 2958, GT-CNRS, 2 rue Marconi, 57070 Metz, France

[2] Georgia Institute of Technology, School of Electrical and Computer Engineering, 30332 Atlanta, U.S.A.

[3] Georgia Tech Europe, 2 rue Marconi, 57070 Metz, France.

[4] King Abdullah University of Science and Technology (KAUST), Advanced Semiconductor Laboratory, Thuwal 23955, Saudi Arabia.

[5] Institute Lafayette, 2 rue Marconi, 57070 Metz, France.

Abstract:

Solid state semiconductor based neutron detectors have the potential to be energy efficient and compact, making them suitable for applications where low power consumption and size constraints are important considerations. In this study, we demonstrate neutron detection devices based on PIN structures consisting of BGaN/GaN superlattice (SL). These SL structures enable us to incorporate significant boron (B) content and achieve good crystalline quality epilayers crucial for better neutron detection. Further, by leveraging the built-in electric field generated by the PIN structure, these devices can be operated without any applied bias, simplifying the overall operation and enabling a more compact size system for detection. Their performance was evaluated by measuring real time current response under neutron irradiation (I_N) and without it (I_D). The neutron induced current density ($\Delta J=J_N - J_D$) was determined, reaching an impressive value of 0.67 pA/cm^2 (2 times J_D) under a thermal neutron flux of 1.2x10^4 n/cm^2/s without biasing, demonstrating their self-powered capability. They exhibit a linear response to varying thermal neutron flux levels. Additionally, the detectors successfully detected low thermal neutron fluxes down to 300 n/cm^2/s, showcasing their potential for diverse applications, including in low neutron environments, screening nuclear warheads, and preventing illegal trafficking of radiological materials.

Introduction:

Neutron detectors are essential tools in various fields, including particle physics, nuclear power plants, and the detection of fissile materials. Currently, one of the most widely used type of neutron detectors is the helium-3 (^{3}He) gas tube detector, which has high thermal neutron capture cross-section (5333 barns), leading to good detection efficiency, typically around 70% and effective discrimination of gamma-ray signals [1], [2]. However, these detectors have several drawbacks, including high operating voltages (>1000 V), the need for high pressurization, large size, and the rarity of ^{3}He gas. As a result, there is a need for the development of smaller, more portable neutron detectors with low power consumption and low cost.

Semiconductor based neutron detectors offer a promising solution to this challenge. Semiconductor materials need to have certain desirable properties to act as neutron detectors such as large bandgap, high resistivity, small electron-hole pair energy, good crystalline quality material, low dielectric constant, high radiation hardness, and high thermal conductivity [3].

Silicon based detectors are typically made using electronic devices (such as PN junctions) coated with a neutron-reactive material [4], such as ^{10}B, or by etching small channels into the semiconductor substrate and backfilling them with a neutron reactive material [5]–[7]. These detectors can have efficiency levels ranging from 5% to as high as 48%, but they suffer from low radiation hardness [8] and require a complex fabrication process.

Among the family of wide bandgap semiconductors, Gallium Nitride (GaN) holds potential as a material for neutron detection [9]–[11]. Despite its appeal, GaN displays limited neutron sensitivity due to its low thermal neutron capture cross-section of 49.6 barns and 3.02 barns for Ga and N respectively. The study of hexagonal Boron Nitride (h-BN) as a neutron detector material has gained traction due to its exceptional properties, such as a large bandgap that reduces thermal noise, the capability to detect thermal neutrons, high resistivity resulting in low leakage current, operational efficiency at elevated temperatures, and robust radiation hardness [12]–[18]. The composition of natural B consists of 20% ^{10}B isotopes and 80% ^{11}B isotopes, which exhibit distinct thermal neutron capture cross-sections of 3840 barns and 570 barns, respectively. Upon capturing a thermal neutron, h-BN undergoes a nuclear reaction, resulting in the formation of lithium (Li) atoms and alpha (α) particles [19] with substantial kinetic energy ($^{10}B + 1n = {}^{7}Li + {}^{4}\alpha$) . These energetic particles generate electron-hole pairs, which are then collected for neutron detection. However, the limited diffusion length of Li and α particles (2-5 μm) hinders with the adequate

generation of electron-hole pairs in the semiconducting material. Hence, it is necessary to use thicker layers of h-BN in device fabrication to effectively absorb neutrons, thereby generating higher numbers of electron-hole pairs that can be collected for neutron detection. However, the growth of thick h-BN layers with excellent crystalline quality poses a significant challenge in device fabrication [2].

BGaN alloys offer a highly promising solution to overcome the limitations discussed earlier. This unique combination takes advantage of the natural B atoms in BGaN, which results in a significant enhancement in thermal neutron detection efficiency compared to GaN. Moreover, BGaN based neutron detection devices feature low thermal noise, thanks to its wide bandgap and reduced sensitivity to gamma rays due to its lighter atomic mass. Additionally, the charge collection efficiency in BGaN is higher compared to h-BN, due to its superior crystalline quality of epilayers, providing enhanced sensitivity to thermal neutron detection. The versatility of BGaN has been demonstrated in various applications, including highly sensitive and high gain UV photodetectors [20], NO_2 gas detectors [21], high electron mobility transistors [22], and Bragg reflectors [23].

In 2014, Atsumi et al. [16] proposed the use of a BGaN Schottky diode with 1.2% B content and a 30 nm thick depletion layer at applied bias of 3 V for neutron detection. The device was found to be sensitive to thermal neutrons, but the signal produced was low due to the low B content in the BGaN layer (1.2%) and the low thickness of the depletion region. Recently, Nakano et al. [24] reported an improvement in the neutron detection efficiency of PIN BGaN diodes by using trimethylboron (TMB) as a B source and growing a 5 μm thick BGaN layer. However, the resulting signal intensity was still low due to the deterioration of the crystalline quality of the thick BGaN layer. These results present promising opportunities for improvement and development of high-efficiency, robust BGaN neutron detectors.

To develop a highly sensitive neutron detector, it is necessary to increase both the B content in the BGaN layer and the thickness of the BGaN layer. Because BN and GaN binary compounds have large structural dissimilarities, it is quite difficult for the $B_xGa_{1-x}N$ alloy to be grown in a broad range of composition. It has been reported that at the typical growth temperature for $B_xGa_{1-x}N$ (about 1000°C) the phase diagram contains regions of spinodal decomposition or phase separation in the interval of $0.028 < x < 0.995$. Furthermore, attempts to increase B content in

thicker BGaN layers lead to surface accumulation of B atoms during growth. This accumulation facilitates strain relaxation through crack formation [25], [26], thereby causing a degradation of overall crystalline quality. To address this issue, we grow BGaN using SL structure, which consist of alternating thin layers of BGaN and GaN, based on semi-bulk approach used by our group to grow thick InGaN layers [27]. The SL structure allows us to have higher incorporation of B atoms (substitutional with Ga) while maintaining good structural quality (low defects density) of the active region which is paramount for achieving high CCE (charge collection efficiency) from the sensing device.

From the application viewpoint, neutron detectors that operate without an externally applied bias have some special advantages, such as simple operation procedure, small size of the detection setup, and suitability for use in extreme conditions (in space, in the nuclear reactor chamber, etc.). In the PIN configuration, the cloud of electron-hole pairs generated through the nuclear reaction between B atoms and thermal neutrons are driven to the electrodes by the presence of built-in electric field to produce an electric signal, thus eliminating the need for any applied bias to drive the device.

In this study, we fabricated a PIN structure consisting of alternating BGaN/GaN epilayers, with nominal B content of 3% in each BGaN/GaN stack and thickness of 20 nm for each layer (40 nm for each stack), resulting in a total SL thickness of 440 nm acting as a primary active layer for neutron detection. This is significantly less than the typical thickness of few micrometers [24] usually needed for BGaN based neutron detectors. For the first time, we evaluated the potential of self-powered operation of PIN BGaN/GaN SL devices based thermal neutron detectors, which are operated by utilizing the built-in electric field generated by the PIN structure and successfully demonstrated their remarkable potential for thermal neutron detection [28]. The figure of merit used for evaluating the performance of these devices was sensitivity (S), defined as $(J_N-J_D)/F = \Delta J/F$, where J_N , J_D are current densities with and without neutron irradiation respectively and F is the incident thermal neutron flux on the detector. The value of S calculated for these devices was $5.58x10^{-5}$ pA/(n/s) corresponding to thermal neutron flux of $1.2x10^4$ n/cm^2/s, indicating their capacity to extract the potential of BGaN based neutron detectors and playing a vital role in the advancement of neutron detection technology.

Materials and Methods:

The BGaN/GaN SL structures were grown by metalorganic vapor phase epitaxy (MOVPE) using a T-shaped reactor [29] at 1000°C. The growth was carried out in a nitrogen (N_2) atmosphere, using trimethylboron (TEB), trimethylgallium (TMG), and ammonia (NH_3) as the sources for of B, Ga and N_2 respectively. This study used a n-type doped GaN standard template (STN) having an average threading dislocation density (TDD) of $5x10^8$ cm^{-2} and a carrier concentration of $3x10^{18}$ cm^{-3}. The details of the growth conditions, B incorporation, and morphology of the films are described in previous work [25], [26]. The BGaN/GaN SL consisted of 20 nm thick BGaN layer and 20 nm thick GaN layer, repeated a total of 11 times. To form the PIN structure, a 300 nm thick layer of p-type GaN was grown on top of the BGaN/GaN SL using MOVPE in an Aixtron Close Coupled Showerhead (CCS) 3×2" reactor in a hydrogen environment at high temperature of 1220°C and at pressure of 85 mbar. Biscyclopentadienyl magnesium (Cp_2Mg) was used as a dopant source, and the film was annealed at 1010°C for 20 minutes to activate the dopant. The structural properties of the samples were characterized using high-resolution X-ray diffraction (HR-XRD) which was performed by Panalytical X'pert Pro MRD system with Cu-Kα radiation in a three-axis mode and the morphological features were examined using a scanning electron microscope (SEM). The compositional content of the sample was analyzed using secondary ion mass spectrometry (SIMS). A standard photolithography based process was used to fabricate the PIN BGaN/GaN SL devices (figure 1). First, devices were isolated by the mesa etch performed using inductively coupled plasma with BCl_3/Cl_2/Ar chemistry. Ti/Al/Ni/Au and Ni/Au stacks were used for the n-contact and the p-contact, respectively. All metal layers were deposited by electron beam metallization. The n-contact was annealed at 850°C for 30s under N_2. The p-contact was annealed at 600°C for 60s under an O_2/N_2 atmosphere.

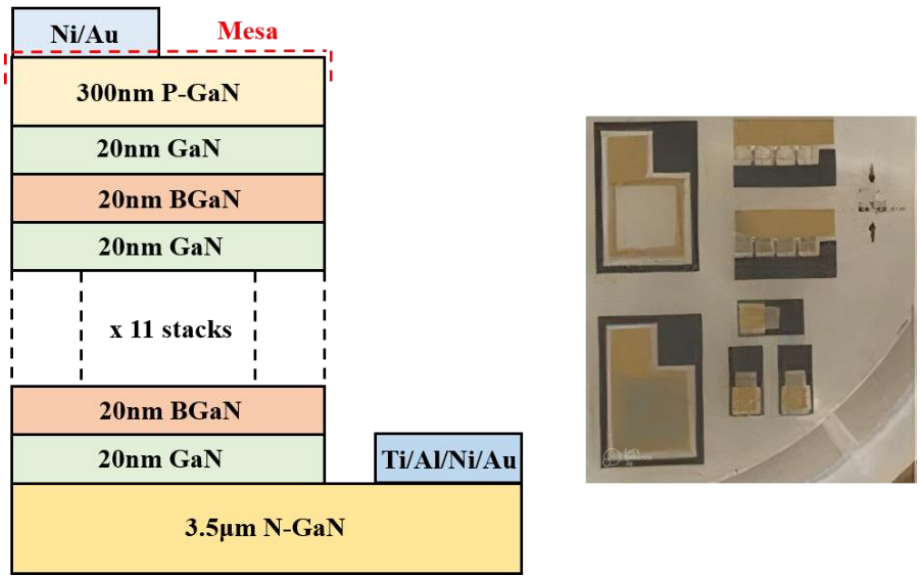

Figure 1: Schematic Diagram and Optical Image of PIN BGaN/GaN SL Device after process.

Neutron irradiation of the devices was performed at Centre Etudes Nucléaires de Bordeaux-Gradignan (CENBG). The neutron source used in this study was a LiF/Cu target that was irradiated with a proton beam, producing neutrons with an energy of 500 KeV. Thermal neutrons were generated by inserting a 5 cm thick high density polyethylene (HDPE) slab between the detector and the target. The HDPE plate was placed at a distance of 1 cm from both the target and the devices being tested (figure 2), resulting in a thermal neutron flux of 1.2×10^4 n/cm^2/s with neutron energies below 1 eV. The current voltage (I-V) characteristics of the devices were measured at room temperature before, during, and after neutron irradiation using a Keithley 2636B source measure unit.

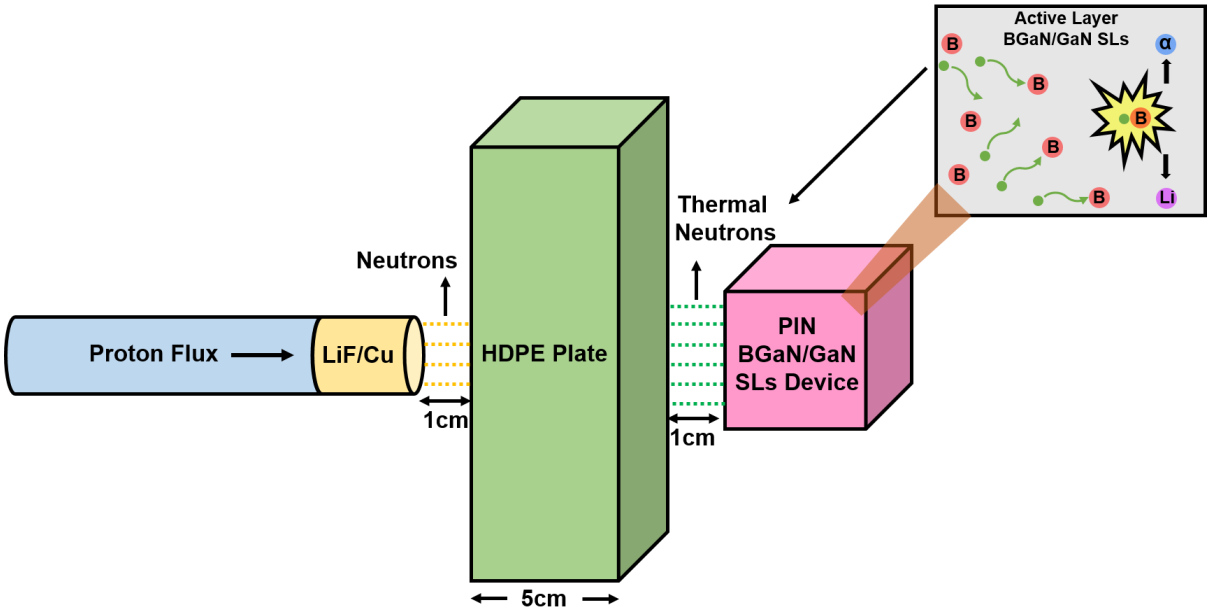

Figure 2: The experimental setup for neutron detection included an HDPE slab placed in front of the LiF/Cu target, with the distance from the LiF/Cu target to the detector being 7 cm.

Results and Discussion:

Surface Morphology and HR-XRD of PIN BGaN/GaN SL Devices

SEM was utilized to examine the morphology of the samples, as depicted in figure 3a. The SEM image reveals a smooth surface with no contaminants or particles present. The samples were also found to be optically transparent (as shown in the inset of figure 3a). The crystallographic properties of the SL structure on STN was analyzed using HR-XRD in the 2θ-ω configuration. The results, shown in figure 3b, exhibit intense GaN peaks and satellite peaks corresponding to BGaN SL, indicating good periodicity and sharp interfaces. However, the satellite peaks are not well pronounced, which may be due to B accumulation at the surface of the BGaN layer, resulting in rougher interfaces. Simulation was performed to estimate the B content and thickness of the BGaN/GaN period, yielding a total thickness of 38±2 nm and a nominal B content of 2.8%. These values were later compared with SIMS analytical data. In addition to the GaN and BGaN related peaks, a diffraction peak for the p-GaN layer is also observed, confirming the successful growth of the PIN device.

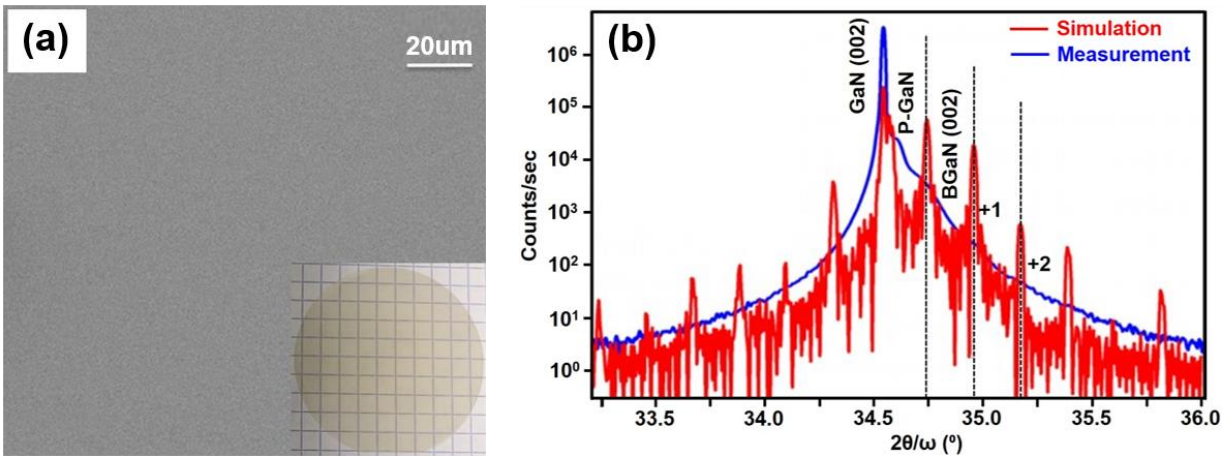

Figure 3: (a) SEM Image and (b) HR-XRD of PIN BGaN/GaN SL Device. Inset in (a) is the photograph of the as-grown sample.

SIMS Analysis of the PIN BGaN/GaN SL Devices

The B concentration in the BGaN layers was characterized using SIMS. Figure 4a shows the depth dependent B and Ga concentrations, which vary in antiphase, indicating the formation of a ternary alloy through the substitution of B atoms for Ga atoms on the III sites of the lattice. The 11 period BGaN/GaN SL structure exhibits good uniformity. In the case of the PIN structure (shown in figure 4b), the average magnesium (Mg) concentration in the p-GaN layer is $3x10^{19}$ atoms/cm^3 and the silicon (Si) concentration in n-GaN is $2x10^{18}$ atoms/cm^3. In the active region (consisting of BGaN/GaN SL), the dopant concentration (Mg and Si) is below the detection limit of SIMS. However, a Si spike is observed at the interface between the p-GaN and BGaN/GaN SL, likely due to surface contamination prior to the regrowth of the p-GaN layer. The B content was found to be 2.8%, with a total BGaN/GaN period thickness of 37±3 nm, consistent with the HR-XRD data. These grown PIN structures with BGaN/GaN SL were then used to fabricate vertical PIN devices for neutron detection.

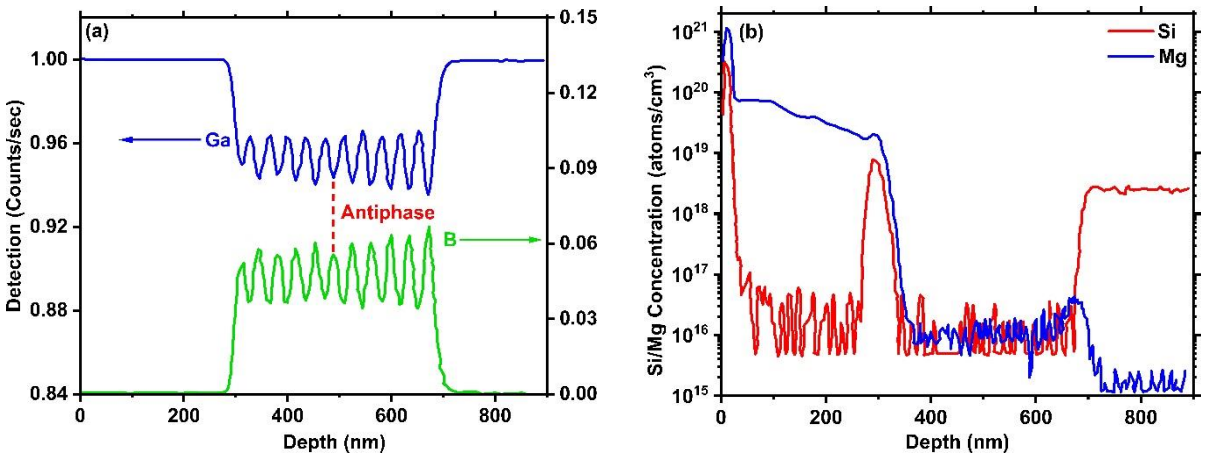

Figure 4: (a) B profile varies anti-phase with Ga and (b) SIMS data of PIN BGaN/GaN SL Device.

J-V Characteristics of PIN BGaN/GaN SL Devices

The electrical properties of the fabricated PIN BGaN/GaN SL devices with an area of 0.6 cm^2 were evaluated using dark current density voltage (J-V) measurements in the range of -2 V to 2 V, and the corresponding current densities calculated from the measurement are shown in figure 5. The device displayed a rectifying J-V curve, with a current density that was four orders of magnitude higher at forward bias compared to reverse bias. At reverse bias, the leakage current density was approximately 4.24 μA/cm^2 at -2 V, but it did not saturate as an ideal diode would, instead continuing to increase with increasing reverse bias voltage. This suggests the presence of leakage current paths related to deep defect levels in the depletion layer. In addition, a small leakage current density of 160 pA/cm^2 was observed at 0.01 V, indicating the potential for detecting a small increase in current density in the device under neutron irradiation.

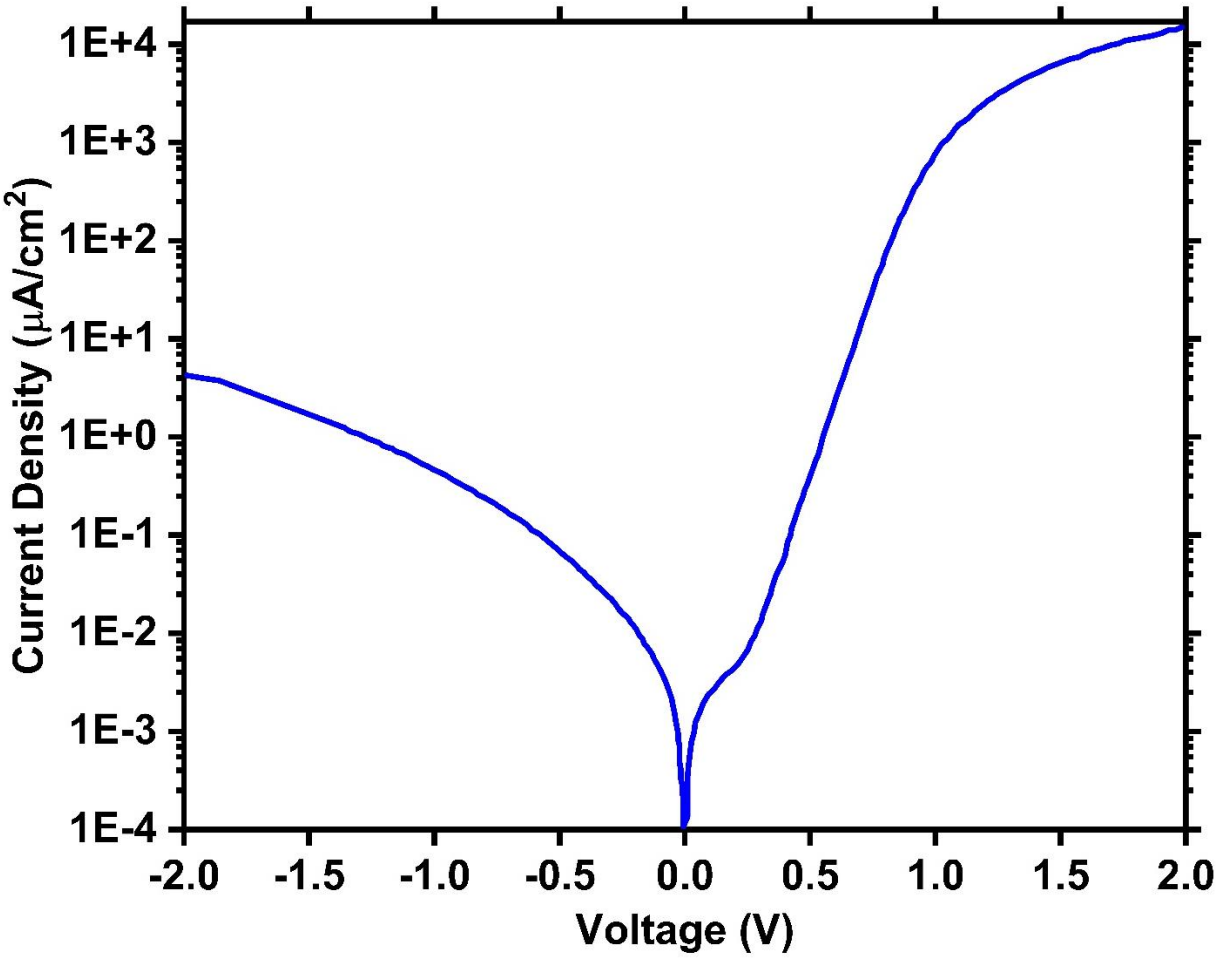

Figure 5: I-V characteristics of PIN BGaN/GaN SL Device under dark condition measured using Keithley 2636B source unit.

Neutron Detection Results of PIN BGaN/GaN SL Devices

The PIN BGaN/GaN SL devices were subjected to four different thermal neutron flux irradiation. To evaluate the sensitivity of the devices, the real time neutron response in terms of change in current density (ΔJ) was plotted as a function of the incident thermal neutron fluxes (figure 6) under no applied bias condition. The inset in figure 6 demonstrate the real time current response corresponding to the four ON/OFF cycles of neutron irradiation which were consistent and repeatable for different thermal neutron fluxes. The observed significant increase in current density for all thermal neutron fluxes was measured without the use of any external electrical amplifier, which has been previously required for BGaN based neutron detectors. This remarkable outcome undeniably demonstrates the self-powered capability of these neutron detectors. The

calculation of S from the detector response in figure 6 yields a value of 5.58×10^{-5} pA/(n/s) corresponding to a thermal neutron flux of 1.2×10^{4} n/cm^2/s, indicating the high sensitivity of the PIN BGaN/GaN SL devices for neutron detection. Additionally, the linear response observed across varying flux levels (represented by the dotted line in Figure 6) suggests excellent device reliability. By extrapolating the linear behavior, the minimum detectable thermal neutron flux using these devices was estimated to be approximately 240 n/cm^2/s. This value is significantly lower than the standard value of thermal neutron flux generally used for characterizing neutron detector devices (~10^4 n/cm^2/s), indicating their capability to be used in low neutron detection environments.

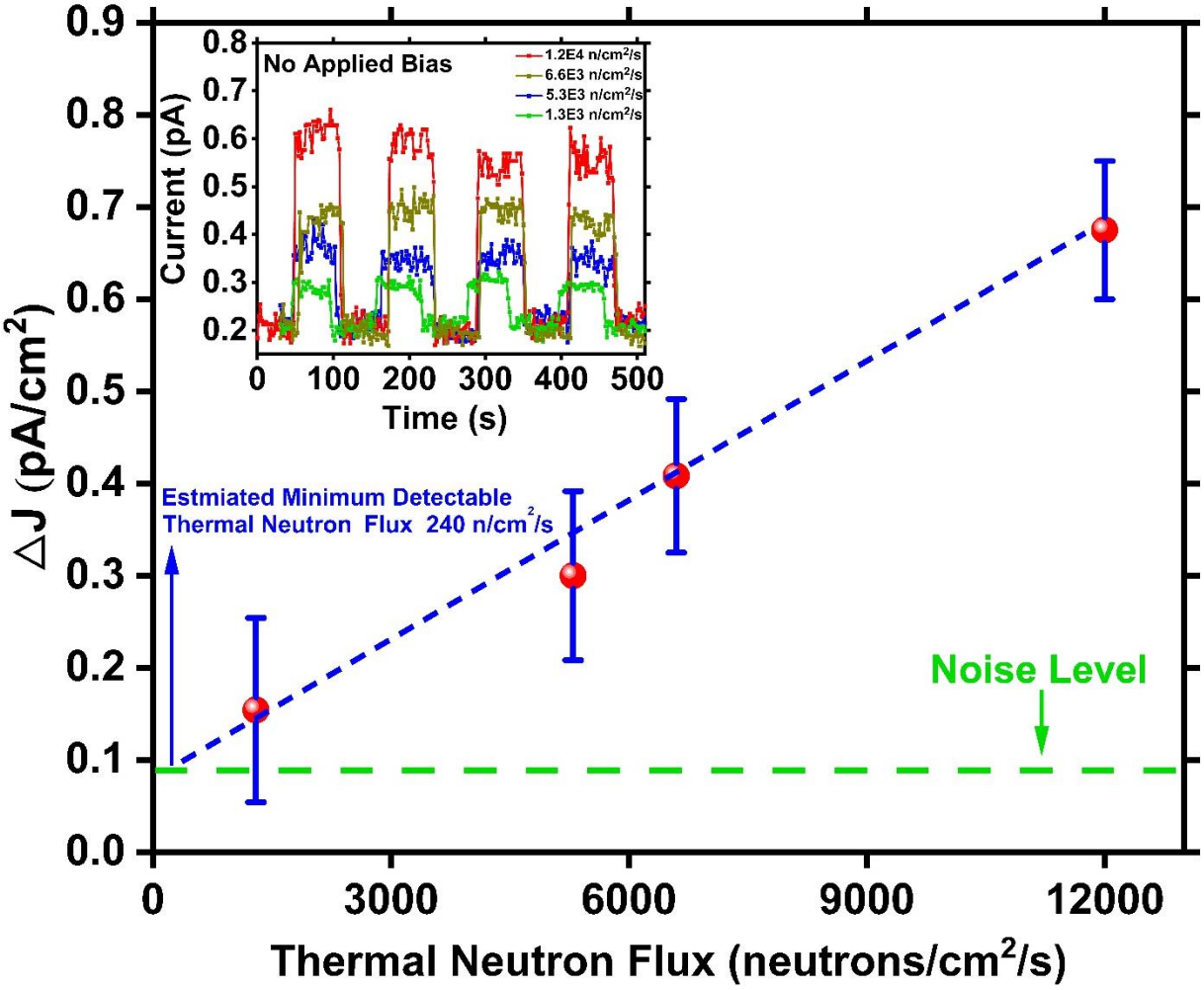

Figure 6: Change in Current Density Vs Incident Thermal Neutron Flux for PIN BGaN/GaN SL Devices. The inset shows the real time measurement of current under four different incident thermal neutron flux irradiation.

Neutron Detection Limit of PIN BGaN/GaN SL Devices

To experimentally validate the estimated value of the minimum detectable thermal neutron flux for the PIN BGaN/GaN SL devices, the real time current response of the device was measured as the incident thermal neutron flux was continuously and gradually decreased. The corresponding current density as a function of time is presented in figure 7. A gradual decrease in the neutron induced current density from 0.50 pA/cm^2 to 0.33 pA/cm^2 was observed, corresponding to the dark current density level in the device. Subsequently, the incident thermal neutron flux was then gradually increased until a clear response ($\Delta J \sim 0.09$ pA/cm^2) was again detected from the device. This value of incident thermal neutron flux corresponds to 300 n/cm^2/s, representing the experimentally measured detection limit of the device. This value is in good agreement with the estimated value previously calculated based on the linear response observed in Figure 6.

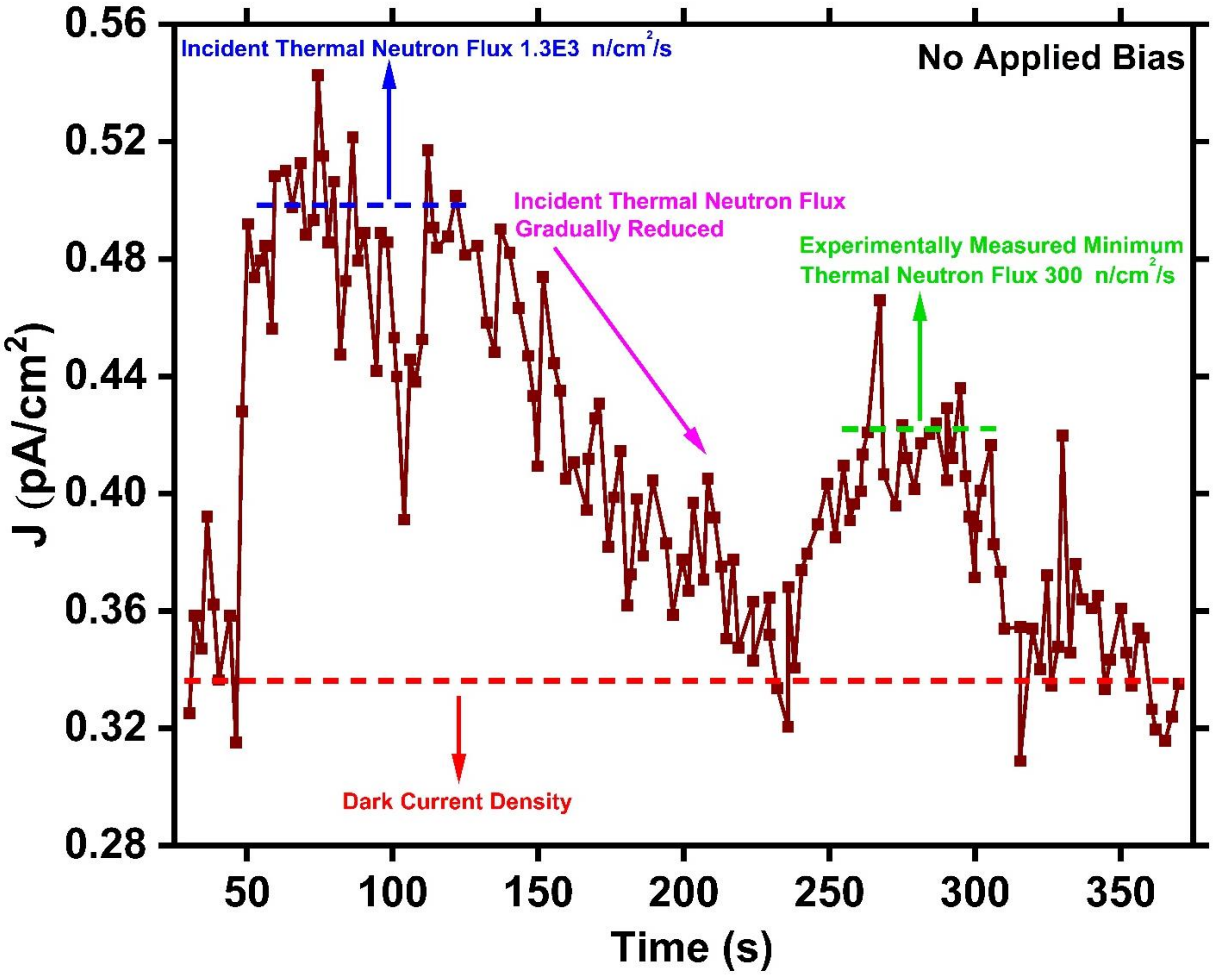

Figure 7: Thermal Neutron Flux Detection Limit of the PIN BGaN/GaN SL devices.

Conclusion

In summary, we used MOVPE to grow PIN BGaN/GaN SL based structures for neutron detection with a nominal B content of approximately 3% in each BGaN/GaN stack. Under no applied bias voltage condition, measurable neutron induced current density was detected in the PIN devices, demonstrating the potential for these thermal neutron detectors. These detectors showed a high sensitivity to thermal neutrons with good linear response under different incident thermal neutron fluxes. The detection limit for thermal neutron flux was determined to be as low as 300 n/cm^2/s. This work represents significant progress towards the development of low cost BGaN based thermal neutron detectors. Overall, these devices show promise as candidates for thermal neutron detection applications and may pave the way for the development of a new class of thermal neutron detector devices.

References

[1] D. S. McGregor, T. C. Unruh, and W. J. McNeil, "Thermal neutron detection with pyrolytic boron nitride," *Nucl. Instruments Methods Phys. Res. Sect. A Accel. Spectrometers, Detect. Assoc. Equip.*, vol. 591, no. 3, pp. 530–533, 2008.

[2] J. Li, R. Dahal, S. Majety, J. Y. Lin, and H. X. Jiang, "Hexagonal boron nitride epitaxial layers as neutron detector materials," *Nucl. Instruments Methods Phys. Res. Sect. A Accel. Spectrometers, Detect. Assoc. Equip.*, vol. 654, no. 1, pp. 417–420, 2011.

[3] F. Nava, G. Bertuccio, A. Cavallini, and E. Vittone, "Silicon carbide and its use as a radiation detector material," *Meas. Sci. Technol.*, vol. 19, no. 10, p. 102001, Aug. 2008.

[4] T. D. Cradduck, "Fundamentals of scintillation counting," *Semin. Nucl. Med.*, vol. 3, no. 3, pp. 205–223, 1973.

[5] M. Wielunski *et al.*, "Study of the sensitivity of neutron sensors consisting of a converter plus Si charged-particle detector," *Nucl. Instruments Methods Phys. Res. Sect. A Accel. Spectrometers, Detect. Assoc. Equip.*, vol. 517, no. 1, pp. 240–253, 2004.

[6] Y Danon *et al.*, "Towards high efficiency solid-state thermal and fast neutron detectors," *J. Instrum.*, vol. 7, no. 03, p. C03014, 2012.

[7] R. Dahal *et al.*, "Self-powered micro-structured solid state neutron detector with very low

leakage current and high efficiency," *Appl. Phys. Lett.*, vol. 100, no. 24, p. 243507, Jun. 2012.

[8] H. Kitaguchi, H. Miyai, S. Izumi, and A. Kaihara, "Silicon semiconductor detectors for various nuclear radiations," *IEEE Trans. Nucl. Sci.*, vol. 43, no. 3, pp. 1846–1850, 1996.

[9] M. Sugiura *et al.*, "Study of radiation detection properties of GaN pn diode," *Jpn. J. Appl. Phys.*, vol. 55, no. 5S, p. 05FJ02, 2016.

[10] C. Zhou, A. G. Melton, E. Burgett, N. Hertel, and I. T. Ferguson, "Neutron detection performance of gallium nitride based semiconductors.," *Sci. Rep.*, vol. 9, no. 1, p. 17551, Nov. 2019.

[11] J. Wang, P. Mulligan, L. Brillson, and L. R. Cao, "Review of using gallium nitride for ionizing radiation detection," *Appl. Phys. Rev.*, vol. 2, no. 3, p. 31102, Sep. 2015.

[12] T. C. Doan, J. Li, J. Y. Lin, and H. X. Jiang, "Growth and device processing of hexagonal boron nitride epilayers for thermal neutron and deep ultraviolet detectors," *AIP Adv.*, vol. 6, no. 7, p. 75213, Jul. 2016.

[13] A. Maity, S. J. Grenadier, J. Li, J. Y. Lin, and H. X. Jiang, "Hexagonal boron nitride neutron detectors with high detection efficiencies," *J. Appl. Phys.*, vol. 123, no. 4, p. 44501, Jan. 2018.

[14] A. Maity, S. J. Grenadier, J. Li, J. Y. Lin, and H. X. Jiang, "High sensitivity hexagonal boron nitride lateral neutron detectors," *Appl. Phys. Lett.*, vol. 114, no. 22, p. 222102, Jun. 2019.

[15] A. Maity, S. J. Grenadier, J. Li, J. Y. Lin, and H. X. Jiang, "High efficiency hexagonal boron nitride neutron detectors with 1 cm2 detection areas," *Appl. Phys. Lett.*, vol. 116, no. 14, p. 142102, Apr. 2020.

[16] K. Atsumi, Y. Inoue, H. Mimura, T. Aoki, and T. Nakano, "Neutron detection using boron gallium nitride semiconductor material," *APL Mater.*, vol. 2, no. 3, p. 32106, Mar. 2014.

[17] A. Mballo *et al.*, "Natural Boron and 10B-Enriched Hexagonal Boron Nitride for High-Sensitivity Self-Biased Metal–Semiconductor–Metal Neutron Detectors," *ACS Omega*, vol. 7, no. 1, pp. 804–809, Jan. 2022.

[18] S. Hasan and I. Ahmad, “Progress in Hexagonal Boron Nitride (h-BN)-Based Solid-State Neutron Detector,” *Electron. Mater.*, vol. 3, no. 3, pp. 235–251, 2022.

[19] S. Majety, J. Li, X. K. Cao, R. Dahal, J. Y. Lin, and H. X. Jiang, “Metal-semiconductor-metal neutron detectors based on hexagonal boron nitride epitaxial layers,” in *Proc.SPIE*, 2012, vol. 8507, p. 85070R.

[20] J. P. Salvestrini *et al.*, “Tuning of internal gain, dark current and cutoff wavelength of UV photodetectors using quasi-alloy of BGaN-GaN and BGaN-AlN superlattices,” in *Proc.SPIE*, 2012, vol. 8268, p. 82682S.

[21] C. Bishop *et al.*, “Highly sensitive detection of NO2 gas using BGaN/GaN superlattice-based double Schottky junction sensors,” *Appl. Phys. Lett.*, vol. 106, no. 24, p. 243504, Jun. 2015.

[22] V. Ravindran *et al.*, “Dual-purpose BGaN layers on performance of nitride-based high electron mobility transistors,” *Appl. Phys. Lett.*, vol. 100, no. 24, p. 243503, Jun. 2012.

[23] M. Abid *et al.*, “Blue–violet boron-based Distributed Bragg Reflectors for VCSEL application,” *J. Cryst. Growth*, vol. 315, no. 1, pp. 283–287, 2011.

[24] T. Nakano *et al.*, “Effective neutron detection using vertical-type BGaN diodes,” *J. Appl. Phys.*, vol. 130, no. 12, p. 124501, Sep. 2021.

[25] A. Ougazzaden, S. Gautier, C. Sartel, N. Maloufi, J. Martin, and F. Jomard, “BGaN materials on GaN/sapphire substrate by MOVPE using N2 carrier gas,” *J. Cryst. Growth*, vol. 298, pp. 316–319, 2007.

[26] S. Gautier *et al.*, “Deep structural analysis of novel BGaN material layers grown by MOVPE,” *J. Cryst. Growth*, vol. 315, no. 1, pp. 288–291, 2011.

[27] K. Pantzas *et al.*, “Semibulk InGaN: A novel approach for thick, single phase, epitaxial InGaN layers grown by MOVPE,” *J. Cryst. Growth*, vol. 370, pp. 57–62, 2013.

[28] A. Mballo, “Neutron detectors based on boron nitride and its alloys,” Université de Lorraine, 2021.

[29] A. Mircea, A. Ougazzaden, and R. Mellet, *Prog. Cryst. Growth Charact.*, 1st ed. 1989.